# Numerical Investigation of AC Loss in HTS Bulks Subjected to Rotating Magnetic Fields

Wafa Ali Soomro, *Member, IEEE*, Youguang Guo, *Senior Member, IEEE*, Hai Yan Lu, *Senior Member, IEEE*, Jian Guo Zhu, *Senior Member, IEEE*, Jian Xun Jin, *Senior Member, IEEE*, and Boyang Shen, *Member, IEEE*

***Abstract*—High-temperature superconductor (HTS) bulks have shown very promising potential for industrial applications due to their highly attractive superconducting characteristics. The practical application, however, has been handicapped by the AC losses. In rotating electrical machines, the magnetic field is a combination of alternating and rotating fields. All the AC loss studies presented in the literature so far have only focused on the alternating AC loss due to the unavailability of experimental techniques and analytical models. This paper present a numerical investigation of AC loss by using the H-formulation under various two dimensional rotating magnetisations with the magnetic flux density vectors rotating in clockwise and anti-clockwise directions in the *XOY*, *XOZ*, and *YOZ* planes. The modeling results show that the rotational AC loss of HTS bulk material is significantly higher than the alternating AC loss.**

***Index Terms*—High-Temperature Superconductor (HTS), AC loss, AC loss measurement, Rotating Magnetic Fields, H-formulation.**

## I. Introduction

Ever since the discovery of high-temperature superconductors (HTS) in 1986, HTS bulks and tapes have shown promising possibilities of high-performance industrial applications after continuous development over three decades. Higher critical temperatures of HTS has triggered the use of HTS material in various large-scale electrical applications [1]. HTS bulks have the ability to trap much higher magnetic fields compared to the traditional permanent magnets [2]. This characteristic makes them attractive for widespread industrial applications such as compact, lightweight, and energy-efficient electrical machines having outstanding high power densities [3, 4]. These applications may range from high-performance electrical motors [5] to HTS magnetic levitation [6]. Conversely, the use of HTS in power system applications is problematic due to dissipative interactions that occur during the exposure of the superconductor to an alternating magnetic fields. This phenomenon is referred to as superconducting alternating current (AC) loss, which is produced due to the movement of vortices inside the superconducting material [7]. The AC loss in HTS bulks can significantly affect the efficiency and economic feasibility of superconducting machines [8]. Moreover, the AC loss can decay and possibly erase the magnetic fields trapped inside the material [9].

In a rotating machine, the magnetic field produced inside the machine can be a combination of alternating and rotating magnetic fields. This scenario may lead to the situation where HTS bulks are exposed to such rotating magnetic fields, which may further accentuate the AC losses. It should be noted that all the previous investigations on AC losses in HTS material were focused on the magnetic fields produced through transport current within HTS or through one dimensional (1D) external excitations. Therefore, the impact of the rotating magnetic fields on HTS AC loss should also be investigated in order to fully understand the loss mechanism in rotating magnetic fields for the efficient design of HTS rotating machines.

Current HTS AC loss measurement techniques [10] such as the electrical method and colorimetric method are limited to measure the AC loss under 1D alternating magnetic fields. There are some specialized arrangements required for producing the rotating magnetic fields. Some of the studies have been published for hysteresis loss measurement in silicon steel and soft magnetic composite (SMC) materials in two dimentional (2D) rotating fields [11] as well as in three dimensional (3D) rotating fields [12]. Such measurement arrangements, however, become complicated in order to maintain the cryogenic environment for HTS simultaneously. Therefore, the rotating AC losses for HTS bulks are not explicitly reported anywhere in the literature. Numerical models, on the other hand, have the ability to overcome these challenges and can predict the HTS properties including AC losses in various complex structures and under various magnetic excitations. Over the time, the numerical modelling technique has evolved to show strong co-relation with measured values studies [13], but this needs complex software implementation and long computation time.

This paper presents a numerical investigation based on finite element analysis (FEA) for the AC loss in an HTS bulk square sample subjected to various rotating magnetic flux density patterns.

## II. Numerical Model Description

A 3D finite element model was designed for this investigation in COMSOL Multiphysics so that different flux density patterns could be applied along various different axes. A cubic sample of HTS bulk with the geometry of 50x50x5 $mm^3$ was selected for this model as shown in Fig. 1. It was assumed that the HTS bulk sample was already cooled to its critical temperature, and hence, the thermal model was not incorporated.

This model is based on the H-formulation, which is widely used for HTS investigation, which shows strong co-relation with experimental studies [13], and hence, this formulation is being used in the present study. The H-Formulation is the mathematical model having the magnetic field strength H as the dependent variable and was first applied to superconducting applications in 2003 [14]. This model is typically a combination of Maxwell Ampere's Law (1), Faraday's Law (2), Constitutive law (3), Ohm's Law (4), and E-J Power Law (5), as follows:

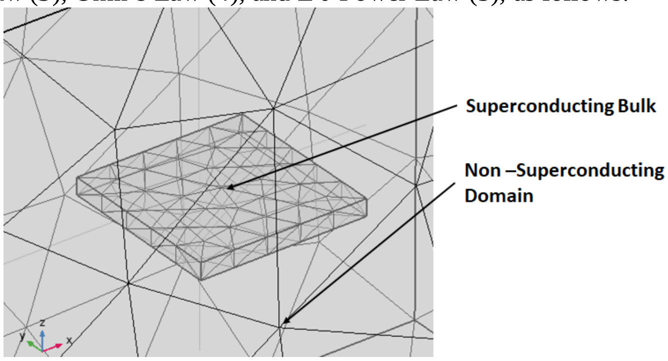


Fig. 1. The geometry of the HTS bulk sample in the model

$$\nabla \times H = J \tag{1}$$

$$\nabla \times E = -\frac{\partial B}{\partial t} \tag{2}$$

$$B = \mu_0 \mu_r H \tag{3}$$

$$E = \rho J \tag{4}$$

where $J$ is the current density, $E$ the electric field strength, $\rho$ the resistivity, $B$ the magnetic flux density, $\mu_0$ the permeability of free space, and $\mu_r$ the relative permeability. For the conventional material, the resistivity is constant in (4), but in terms of superconductors, it depends on the current density. Normally, it assumes the form of power-law:

$$\rho = \frac{E_0}{J}\left(\frac{J}{J_c}\right)^{n-1} \tag{5}$$

where $E_0$ is a characteristic electric field stength, $J_c$ the critical current density, and $n$ represents the steepness of the shift from superconducting to normal state, usually called power factor. As $n$ reaches infinity, the power-law approaches the critical state model [15], which is commonly known as Bean's critical state model. Combining (1)-(5), one obtains the partial differential equation (PDE) in terms of variable $\boldsymbol{H}$ as follows

$$\frac{\partial(\mu_0 \mu_r H)}{\partial t} + \nabla \times (\rho \nabla \times H) = 0 \tag{6}$$

which can be solved in the finite-element program [16].

The external magnetic fields can be set up at the boundary of air domain around the conductor's region by carefully setting the Dirichlet boundary conditions. The same setting can also be implemented for the transport current to the whole region of the conductor. In order to reduce the problem, it is desirable to set symmetric and/or periodic conditions on the domain boundary, which also helps in reducing the computing time.

AC losses can be computed by integrating the power dissipation EJ over the domain of interest and taking the average of one excitation cycle. Usually, it is sufficient to simulate only once cycle by averaging the second half, and this helps avoid the transient behavior in the first half cycle [17].

$$Q = \frac{2}{T}\int_{0.5T}^{T}\int_{\Omega} E \cdot J \, d\Omega dt \tag{7}$$

where $\boldsymbol{\Omega}$ represents the domain for calculating AC loss and T is the period of AC signal. The other relevant parameters used in the model are listed in Table I.

TABLE I
MODEL PARAMETERS

| Symbol | Parameter | Value |
|---|---|---|
| $\mu_0$ | Permeability of free space | $4\pi \times 10^{-7}$ H $m^{-4}$(Unit?) |
| $n$ | Power Factor | 25 |
| $J_c$ | Critical Current Density | $10^3$ A $m^{-2}$ |
| $E_0$ | Characteristic Electric Field | $10^4$ V $m^{-1}$ |
| $A$ | Area of Sample | $12.5\times10^{-6}$ $m^{-3}$ (unit?) |

## III. ROTATING MAGNETIC FIELDS

Typically, in 1D magnetic fields, the magnetic flux density vector $B$ is restrained from flowing along with the direction of the magnetic field strength $H$. However, in rotating electrical machines, the magnetic field is generally rotating in a 2D plane, where **B** and **H** vectors may not be in the same direction.

In this model, the magnetic field is applied to the boundaries of the superconducting domain. In the case of 1D alternating field, a sine wave is introduced with the desired amplitude. However, in the case of 2D rotating magnetisation, the applied rotating magnetic field is simply a set of sine waveforms at the boundaries of two different axes as per the testing criteria, which can be described by

$$B_{1D(alt)} = B_0 \sin(\omega t \pm \emptyset) \tag{8}$$

$$B_{2D(rot)} = \begin{cases} B_0 \sin(\omega t) & (9) \\ B_0 \sin(\omega t \pm \emptyset)\left(1 - \exp\left(-\frac{t}{\tau}\right)\right) & (10) \end{cases}$$

where $B_0$ is the amplitude of magnetic field, $\omega$ the angular frequency, $\emptyset$ represents the phase shift angle, and $\tau$ is the time constant, which is set as 0.05 s. A purely circular rotating field is created which is usually obtained by shifting the phase angle of the second source by 90 degrees (i.e. $\emptyset = \pi/2$). In order to achieve a purely circular magnetic field in a clockwise direction, the phase angle is shifted by +90 degrees ($\emptyset = \pi/2$) and in case of magnetic field rotating in anticlockwise direction, the phase angle is shifted by -90 degrees ($\emptyset = -\pi/2$) as shown in Fig. 2. It must be noted that when a phase angle is shifted along the axis, the initial value of the magnetic field is not equal to zero, which creates a problem of the initial values in FEA, and the model could not be converged. Therefore, an exponential step function is introduced in the second field source in (10) in order to create a transient start.

Various 2D rotating flux density vectors in the *XOY*, *XOZ*, and *YOZ* planes are applied in this investigation in order to see the loss mechanism for both clockwise and anti-clockwise directions at various amplitudes, respectively. Fig. 3 shows the **B** Loci of various flux density patterns used in this study at 1.5 T where a purely circular rotating magnetic field around the sample can be observed.

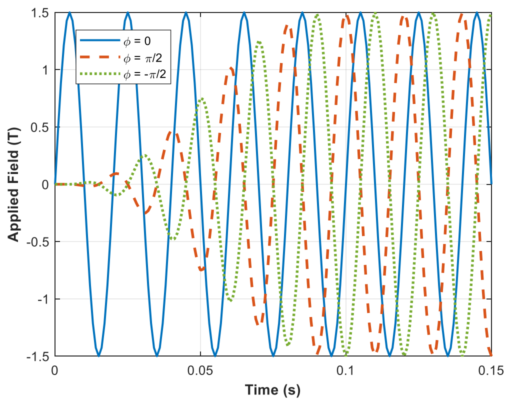


Fig. 2. Applied magnetic field

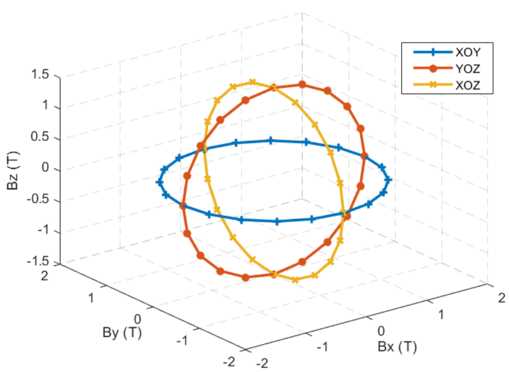


Fig. 3. Loci of flux density for *XOY*, *XOZ*, and *YOZ*

## IV. Results and Discussions

In this study, the magnetization AC loss of a cubic HTS bulk sample of 50x50x5 $mm^3$ has been systematically calculated under various 1D alternating and 2D rotating flux density patterns up to 2 T. Since the rotating magnetic fields are mainly observed in rotating machines and HTS bulk can be a promising candidate for such applications, this investigation has been performed primarily at power frequency (50 Hz).

Initially, the AC loss was obtained for alternating magnetic fields along the x-, y- or z-axis as shown in Fig. 4. It can be seen that the AC loss in the z-direction is much higher than those in the x- and y- directions until 0.1 T, which is a common loss mechanism when HTS samples are subjected to perpendicular fields. However, the difference decreases significantly as the flux density increases up to 2 T. Furthermore, there is a slight difference between the AC losses in the x- and y-axes as well, where the AC loss in the x-axis is slightly higher than that in y-axis in the overall trend except at 0.25 T where the losses in the y-direction are slightly higher due to the anisotropy of HTS.

Fig. 5 shows the AC loss under 2D rotating flux density vectors in the *XOY*, *XOZ*, and *YOZ* planes, respectively. It can be seen that the AC losses in *XOZ* and *YOZ* are clearly higher than that in the XOY plane due to the involvement of the perpendicular field element. However, compared to the 1D AC loss in the z-axis, the 2D loss increases up to two times of the corresponding 1D loss until 0.1 T, and then reduces significantly to negligible difference up to 2 T. Furthermore, the AC loss in *XOY* increases up to 4.2 times at 0.25 T compared to the AC losses at both x- and y-axes, however, the difference is significantly reduced until 2 T, but still, there seems to be a 75% increase.

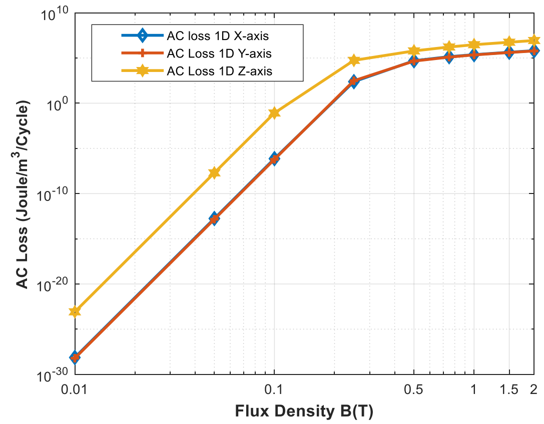


Fig. 4. AC loss under 1D alternating fields.

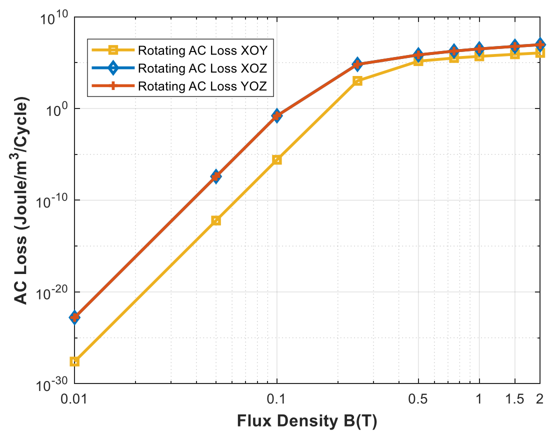


Fig. 5. AC loss under various rotating magnetic flux density patterns.

In the above findings, the rotating losses in the *XOY*, *XOZ*, and *YOZ* planes are reported where the field rotates in the clockwise direction in a circular pattern. Fig. 6 shows a comparison of AC losses in these scenarios when the field rotates in the anti-clockwise direction. The rotating AC losses seem to be the same in both the clockwise and anti-clockwise directions for all three patterns up to 0.1 T, but there seems to be a slight decrease in the loss when the field rotates in the anti-clockwise direction, which continues until 2T. This slight reduction can be associated with the shifting of phase angle by -90 degrees ($\emptyset = -\pi/2$) where the impact of the rotating field appears to be less at the start of each cycle as shown in Fig. 2.

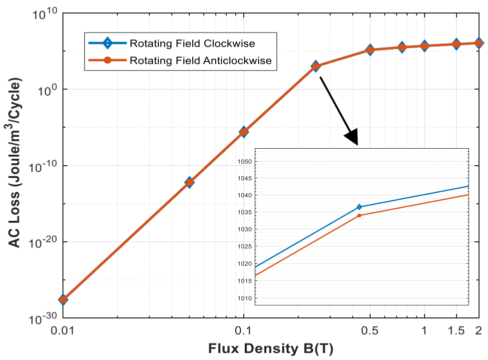


(a)

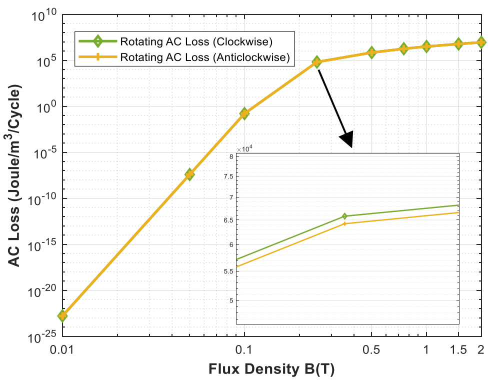


(b)

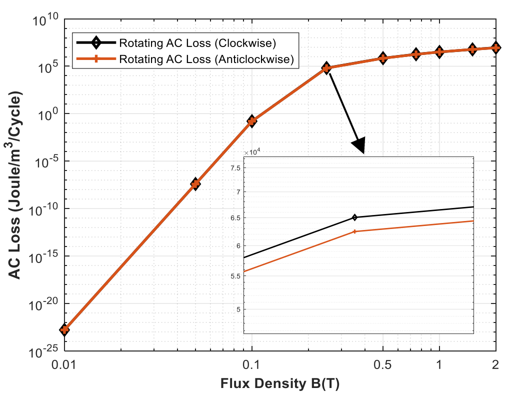


(c)

Fig. 6. Comparison of AC losses with 2D rotating flux density in clockwise and anti-clockwise directions in the (a) *XOY* (b) *XOZ* and (c) *YOZ* planes.

## V. Conclusion

In this study, a systematic investigation on AC loss is performed by numerical modeling technique based on FEA and H-formulation when an HTS bulk sample is subjected to various alternating and rotating flux density patterns up to 2 T. The findings show that the losses are significant until 0.1 T when the magnetic field rotates in the z-axis. However, the losses increase up to four times when the field rotates around the x- or y-axis. Furthermore, there appears to be a slight decrease in the AC loss when the magnetic field rotates in the anti-clockwise direction, compared to the loss subject to the rotating field in the clockwise direction.

This investigation provides an overview and prediction of the AC loss mechanism in rotating magnetic fields as it requires specialized equipment to experimentally validate these results.

In the future work, a testing system shall be developed for the characterization of magnetization properties of HTS under rotating magnetic field in order to measure the rotating AC loss.

## VI. References


[1] J. X. Jin, *et al.*, "Enabling high-temperature superconducting technologies toward practical applications," *IEEE Transactions on Applied Superconductivity,* vol. 24, no. 5, pp. 1-12, 2014, doi: 10.1109/TASC.2014.2346496.

[2] J. H. Durrell, *et al.*, "A trapped field of 17.6 T in melt-processed, bulk Gd-Ba-Cu-O reinforced with shrink-fit steel," *Superconductor Science and Technology,* vol. 27, no. 8, p. 082001, 2014.

[3] D. Zhou, M. Izumi, M. Miki, B. Felder, T. Ida, and M. Kitano, "An overview of rotating machine systems with high-temperature bulk superconductors," *Superconductor Science and Technology,* vol. 25, no. 10, p. 103001, 2012.

[4] R. Bause, M. D. Ainslie, M. Corduan, M. Boll, M. Filipenko, and M. Noe, "Electromagnetic design of a superconducting electric machine with bulk HTS material," *arXiv preprint arXiv:1903.08906,* 2019.

[5] H. Moon, Y. Kim, H. Park, M. Park, and I. Yu, "Development of a MW-class 2G HTS ship propulsion motor," *IEEE Transactions on Applied Superconductivity,* vol. 26, no. 4, pp. 1-5, 2016, doi: 10.1109/TASC.2016.2536660.

[6] L. Zheng, J. Jin, Y. Guo, W. Xu, and J. Zhu, "Performance analysis of an HTS magnetic suspension and propulsion system with a double-sided HTS linear synchronous motor," *IEEE Transactions on Magnetics,* vol. 48, no. 2, pp. 655-658, 2012, doi: 10.1109/TMAG.2011.2174046.

[7] M. D. Ainslie, C. W. Bumby, Z. Jiang, R. Toyomoto, and N. Amemiya, "Numerical modelling of dynamic resistance in high-temperature superconducting coated-conductor wires," *Superconductor Science and Technology,* vol. 31, no. 7, p. 074003, 2018/06/06 2018, doi: 10.1088/1361-6668/aac1d3.

[8] X. Xiao, Y. Liu, J. Jin, C. Li, and F. Xu, "HTS applied to power system: benefits and potential analysis for energy conservation and emission reduction," *IEEE Transactions on Applied Superconductivity,* vol. 26, no. 7, pp. 1-9, 2016, doi: 10.1109/TASC.2016.2594800.

[9] Y. Zushi, I. Asaba, J. Ogawa, K. Yamagishi, and O. Tsukamoto, "AC losses in HTS bulk and their influence on trapped magnetic field," *Cryogenics,* vol. 45, no. 1, pp. 17-22, 2005.

[10] Y. Wang, X. Guan, and J. Dai, "Review of AC loss measuring methods for HTS tape and unit," *IEEE Transactions on Applied Superconductivity,* vol. 24, no. 5, pp. 1-6, 2014.

[11] Y. G. Guo, J. G. Zhu, and J. J. Zhong, "Measurement and modelling of magnetic properties of soft magnetic composite material under 2D vector magnetisations," *Journal of Magnetism and Magnetic Materials,* vol. 302, no. 1, pp. 14-19, 2006/07/01/ 2006, doi: https://doi.org/10.1016/j.jmmm.2005.08.023.

[12] Y. Guo, J. G. Zhu, Z. W. Lin, J. J. Zhong, H. Y. Lu, and S. Wang, "Determination of 3D magnetic reluctivity tensor of soft magnetic composite material," *Journal of magnetism and magnetic materials,* vol. 312, no. 2, pp. 458-463, 2007.

[13] B. Shen, F. Grilli, and T. Coombs, "Review of the AC loss computation for HTS using H formulation," *Superconductor Science and Technology,* vol. 33, no. 3, p. 033002, 2020.

[14] R. Pecher, "3D-modelling of bulk type II superconductors using unconstrained H-formulation," *Proc. 6th EUCAS, Sorrento, Italy, 2003,* 2003.

[15] C. P. Bean, "Magnetization of hard superconductors," *Physical review letters,* vol. 8, no. 6, p. 250, 1962.

[16] B. Shen, *et al.*, "Design and simulation of superconducting lorentz force electrical impedance tomography (LFEIT)," *Physica C: Superconductivity and its Applications,* vol. 524, pp. 5-12, 2016.

[17] B. Shen, *et al.*, "Investigation of AC losses in horizontally parallel HTS tapes," *Superconductor Science and Technology,* vol. 30, no. 7, p. 075006, 2017.